**Supporting Online Material for:**

# Endogenous protein S-nitrosylation in *E. coli*: regulation by OxyR

Divya Seth, Alfred Hausladen, Ya-Juan Wang and Jonathan S. Stamler*

* To whom correspondence should be addressed: Email: jonathan.stamler@case.edu

## This PDF file includes:

## Materials and Methods

### Bacterial Strains and Plasmids

*E. coli* K12 strain MG1655 (F-, *LAM-*, *rph-1*) was obtained from the *E. coli* Genome project, University of Wisconsin-Madison, and the isogenic strain GSO77 (MG1655 *oxyR::kan* derivative) was obtained from Dr. G. Storz *(26)*. The strain BW25113 and the isogenic Δ*oxyR,* Δ*hcp* and Δ*hmp* strains from the Keio collection (*28*) were obtained from the Coli Genetic Stock Center (CGSC) at Yale University. To prepare the plasmid overexpressing OxyR, the gene was PCR-amplified from MG1655 genomic DNA using primers that add a ribosome-binding site to the 5' end of the *oxyR* gene (5'-ATTAGGATCCCTTTAAGAAGGAGATATACATATGAATATTCG-3') and a FLAG tag to the 3' terminus (5'-CGCATAAGCTTTTACTTGTCATCGTCGTCCTTGTAGTCAACCGCCTGTTTTAAAAC -3'). The resulting DNA fragment was cloned into the vector pUC19.

### Reagents

S-nitrosocysteine (CysNO) and S-nitrosoglutathione (GSNO) were prepared as previously described (*29*). All primers were obtained from Integrated DNA technologies (Skokie, IL).

### Bacterial Culture and Manipulations

Bacteria were grown in LB medium or on LB agar plates for cloning and storage. For the various assays, bacteria were grown in MOPS-buffered minimal media containing 80 mM MOPS, 4 mM tricine, 9.95 mM $NH_4Cl$, 0.276 mM $K_2SO_4$, 0.1 mM $CaCl_2$, 0.528 mM $MgCl_2$, 0.01 mM $FeSO_4$ and 50 mM NaCl in MQ water (pH 7.0), as well as 0.013 mM $K_2HPO_4$, 0.2% glucose and trace metals. Ampicillin (100 mg/L) was added when required. Anaerobic bacterial growth was carried out without shaking in a 37°C incubator placed inside a glove box with an atmosphere of 85% $N_2$, 5% $CO_2$ and 10% $H_2$ (Coy Laboratory Products). All culture media, buffers and cultures were equilibrated in the glove box for 18 hr prior to use. Any $O_2$ traces were continuously removed with a palladium catalyst.

Cultures were started by inoculation of the media with 4% of overnight cultures and allowed to grow to mid-log phase (A600 0.3-0.4). Where indicated, sodium nitrate or sodium fumarate solutions were added to the growth media to a final concentration of 10 mM. Some cells were treated with specified concentrations of CysNO or GSNO for 5 min before harvesting. All cells were chilled on ice, harvested by centrifugation and washed once in phosphate buffered saline (PBS, pH 7.4). Pellets were stored at -80$^0$C. For RNA extractions, pellets were stored overnight at 4°C in RNAlater solution (Ambion).

**Measurement of S-nitrosothiols (SNOs) by photolysis-chemiluminescence**

SNO measurements in lysates or purified SNO-OxyR were done using Hg-coupled photolysis/chemiluminescence essentially as described (*30*). Briefly, nitric oxide (NO) released from SNOs by UV-photolysis is detected by chemiluminescence generated by the reaction of NO with ozone. Pre-treatment of samples with $HgCl_2$ (2 mM) or p-chloromercuribenzoic acid (PCMB) (0.5 mM) removes SNOs specifically and allows differentiation between SNOs and other UV-photolyzable bound NO species (denoted XNOs).

**Detection of S-Nitrosylated Proteins (SNO-proteins) by Biotin-Switch or SNO-RAC (Resin-Assisted Capture)**

Total SNO-proteins and OxyR-SNO were detected with the biotin-switch assay (*31*) or by SNO-RAC (*32*) respectively, described briefly here. The biotin-switch assay involves the ascorbate-dependent biotin labeling of SNO-cysteines followed by pulldown by streptavidin agarose. For biotin-switch of lysates, lysate (300 μL; 1-2 mg total protein) was incubated in HEN buffer containing 100 mM HEPES, 1 mM EDTA, 0.1 mM neocuproine (pH 7.7) with SDS (1% final concentration) and the thiol-blocking agent 0.1% methyl methanethiosulfonate (MMTS) (Sigma-Aldrich; St. Louis, MO) in a final volume of 2 ml at 50°C for 20 min. Proteins were acetone precipitated, washed three times in 70% acetone, and resuspended in HEN buffer containing 0.2 mM biotin-HPDP (Pierce; Rockford, IL), with or without 50 mM sodium ascorbate. Samples were incubated at room temperature for 1 hr. and, following acetone precipitation, biotinylated proteins were pulled down using 50 μL streptavidin-agarose beads (Sigma-Aldrich). Total S-nitrosylated proteins were separated by non-reducing SDS-PAGE and transferred to nitrocellulose membranes, and blotted proteins were detected using neutravidin-HRP. Controls included samples not treated with ascorbate and samples subjected to UV-photolysis prior to biotin-switch to remove NO groups.

For SNO-RAC (*32*), OxyR-SNO samples were initially treated as in the biotin-switch method. Following blocking of free thiols with MMTS and acetone precipitation, the pellets were re-suspended in HEN buffer containing 1% SDS. Following the addition of 50 μl thiopropyl sepharose and 50 mM sodium ascorbate, samples were rotated in the dark for 4 hr. The bound proteins were eluted with DTT and FLAG-tagged SNO-OxyR was Western blotted using anti-FLAG antibodies following separation on reducing SDS-PAGE.

**Microarray**

Parental and Δ*oxyR* MG1655 were grown anaerobically on 10 mM nitrate or fumarate and harvested at A600 0.4-0.45. Cultures were treated with RNAprotect bacteria reagent (Qiagen) to stabilize RNA and RNA was extracted with the

RNEasy kit (Qiagen). Further sample preparation, hybridization and processing of the arrays were carried out by the Virginia Bioinformatics Institute at Virginia Tech (Blacksburg, VA). Briefly, cDNA was prepared with random hexamer oligonucleotide primers, biotin-tagged with the Nugen Ovation Pico labeling kit and hybridized to the *E. coli* Genome 2.0 Array (Affymetrix). Binding was measured with fluorescently labeled streptavidin. The microarray data in MIAME compliant form has been submitted (accession number GSE24524). Data were analyzed using GenspringGX software (Agilent) and the genes induced > 2-fold on nitrate (p-value cutoff = 0.05) are shown in Tables S1 and S2.

**Reverse Transcription and Real Time PCR**

RNA was extracted using the Masterpure RNA purification kit (Epicenter Biotechnologies, Madison, WI) and 3 μg of RNA was used for preparing cDNA with random hexamer oligonucleotide primers (Integrated DNA Technologies) using MuMLV reverse transcriptase enzyme (Invitrogen). Gene specific primers were used for real-time PCR in a MyiQ Real-Time PCR Detection System (BioRad) using 2X iQ SYBR green supermix (BioRad). The expression of 16*S* rRNA in each sample was used to normalize the expression of the gene(s) of interest. Real-time PCR primers are listed in Table S4. Fold change in expression was calculated using the comparative $C_t$ method.

**Electrophoretic mobility shift assay**

The LICOR IR-800 labeled *hcp* promoter 347 bp DNA fragment was prepared by PCR amplification of the promoter region using specific primers (5' IR-800-TGCACTGGGCTTATGCGGTGCC-3' and 5' CAGCCGTTTCCTGCCGGAGTACGG-3') and MG1655 genomic DNA as template. Different amounts of OxyR were incubated with 1 pmol of *hcp*-promoter DNA in the presence or absence of 1 pmol *katG* promoter DNA (unlabeled 60 bp DNA encompassing the OxyR-binding site; 5' CCAACAATATGTAAGATCTCAACTATCGCATCCGTGGATTAATTCAATTATAACTTCTCT 3'). The reaction was carried out in a buffer containing 25 mM Tris-Cl pH 7.9, 6.25 mM $MgCl_2$, 10% glycerol, 0.5 mM EDTA, 0.05% NP-40 and 50 mM KCl at room temperature for 10 min in the presence of either 50 μM DTT or GSNO. The samples were separated on a 5% polyacrylamide gel and the bands were visualized on the Odyssey infrared imaging system (LI-COR Inc.).

***In Vitro* Transcription Assay and Primer Extension**

*In vitro* transcription reactions followed by primer extension were performed as described by Storz and Altuvia (*33*). Recombinant OxyR was prepared, reduced and modified to make S-oxidized or S-nitrosylated OxyR as described (*13*).

The stoichiometry of SH, S-Ox and S-NO was ~1mol/mol protein in each case. Plasmid pBT22, which was used as a template for *katG* assays, has a katG-expressing DNA fragment in pAT153 cloned at the HindIII site (a gift from Dr. P. Loewen). For *hcp*, the HindIII fragment in pBT22 was replaced by a DNA fragment containing the *hcp* coding region and the entire intergenic region 5' to it. Primer extension was done using MuMLV reverse transcriptase (Invitrogen) according to the manufacturer's instructions.

**Identification of site of S-nitrosylation in OxyR (see Supplementary Text)**

Two methods were employed to analyze S-nitrosylation of purified OxyR *in vitro*. In both approaches recombinant OxyR was reduced using TCEP-agarose for 1 hr under anaerobic conditions as per manufacturer's instructions. After removal of TCEP-agarose by centrifugation, OxyR was S-nitrosylated by treatment with a 20-fold molar excess of GSNO for 30 min at room temperature and the protein was then acetone precipitated. In the first method, the pellet was resuspended and subjected to SNO-RAC modified by omission of a thiol-blocking agent. Following on-resin trypsinization, the peptides were eluted with 5 mM TCEP, labeled with 15 mM iodoacteamide (IAA) and identified by mass spectrometry (LC-MS/MS). In the second method, SNO-OxyR was prepared as described and free thiols were blocked with 50 mM NEM in HEN buffer containing 1% SDS at 50°C for 20 min. Following acetone precipitation and re-suspension in HEN buffer, IAA labeling was done with 100 mM IAA in the presence or absence of 50 mM ascorbate. The labeled protein was acetone precipitated and trypsin digested before identification of peptides by mass spectrometry (LC-MS/MS; see below).

**Liquid Chromatography and Tandem Mass Spectrometry (LC-MS/MS).** Samples were cleaned using C18 spin columns (Thermo Pierce #89870, Rockford, IL), reconstituted with 0.1% formic acid and analyzed by LC-MS/MS. Separation of peptides via capillary liquid chromatography was performed using a Waters nanoAquity system (Waters Corp., Milford, MA). Mobile phase A (aqueous) contained 0.1% formic acid in 5% acetonitrile and mobile phase B (organic) contained 0.1% formic acid in 85% acetonitrile. Separation was achieved using a C18 column (75 μm × 20 cm, Waters Corp., Ethylene Bridged Hybrid column # BEH300) through a 90 minute gradient of 6% to 45% mobile phase B at a flow rate of 0.30 μL/min. Mass spectrometric analysis was performed using a hybrid linear ion trap Orbitrap Velos mass spectrometer (LTQ-Orbitrap Velos, Thermo, Waltham, MA), operated at a resolution of 60,000. Data-dependent MS/MS scans were performed with inclusion lists, including tryptic peptides containing cysteines with up to one missed cleavage and cysteine alkylation by iodoacetamide (57 Da) and N-ethylmaleimide (125 Da), as well as S-nitrosylation (29

Da) and methionine oxidation (16 Da) (corresponding to approaches with and without SNO-RAC, respectively, as described above).

Search engines of Mascot (Matrix Sciences, Inc.) and MassMatrix (*34*) were applied to process raw LC-MS/MS data. Peptide identification was achieved by searching against the *E. coli* non-redundant database from the National Centre for Biotechnology Information (NCBInr, 1,200,738 sequences, April 5th, 2011). Mass accuracy was limited to 10 ppm for precursor ions and 0.6 Da for product ions, with tryptic enzyme specificity and up to one missed cleavage. Variable modifications included cysteine alkylation by iodoacetamide and N-ethylmaleimide, S-nitrosylation and methionine oxidation. Peptides passed identity threshold with mass accuracy of ≤ 10 ppm and expectation value of $p \leq 0.05$.

**Pulldown with Biotin-Labeled DNA**

The biotin-labeled *hcp* promoter 347 bp DNA fragment was prepared by PCR amplification of the promoter region using specific biotin-labeled primers (5' biotin-TGCACTGGGCTTATGCGGTGCC-3' and 5' biotin-CAGCCGTTTCCTGCCGGAGTACGG-3') and MG1655 genomic DNA as template. Biotin-labeled DNA (25 nM) along with 500 μM DTT or GSNO was added in PBS, pH 7.4, to 300 μg lysate from Δ*oxyR* cells transformed with plasmid overexpressing OxyR-FLAG. The experiment was carried out under anaerobic conditions to prevent the oxidation of OxyR. Following incubation at room temperature for 1 hr, DNA was pulled down using streptavidin-agarose. The beads were washed 5X with PBS, pH 7.4, and the bound proteins were eluted by boiling in Laemmli buffer, separated on SDS-PAGE and Western blotted for both OxyR-FLAG and RNA polymerase β'-subunit.

**Zone of Inhibition Assay**

WT, Δ*hcp*, or Δ*oxyR* cells were grown overnight in MOPS-buffered minimal media. Cells ($10^7$) in 3 ml of top agar (6g/L bacto agar in minimal media) were overlaid onto minimal media agar plates (15 g/L bacto agar). Cups were made in the agar using the tip of a glass Pasteur pipette, and 5 μl of GSNO of specified concentration was added to the cups. Plates were incubated overnight at 37°C and the diameters of the zones of inhibition were then measured. For anaerobic assays, the top agar contained 20 mM nitrate or fumarate, and plates of overlaid cells were equilibrated in the anaerobic chamber at 37°C for at least 4 hours before GSNO treatment and maintained in the chamber until harvested.

**Bacterial Growth Assay**

*E. coli* were sub-cultured in MOPS-buffered minimal medium at 2% inoculum (v/v). Cells (100 μl) were placed in 96-well plates and incubated at 37°C in a Fluostar absorbance plate reader until A600=0.2-0.3. GSNO or hydrogen peroxide (100μl, prepared in MOPS-buffered minimal medium to achieve indicated concentrations) was added, and A600 was measured every 15 min.

**Macrophage Survival Assay (Δ*hcp*)**

Murine macrophage (RAW 264.7) cells were grown in 96-well plates and stimulated with LPS (100 ng/ml), IFNγ (100 Units/ml) and L-arginine (1 mM) for 18 hr. The iNOS inhibitor 1400W was used at 100 μM. Log-phase WT and Δ*hcp* bacteria were added at a multiplicity of infection (MOI) of 10 and incubated at 37°C for 30 min. Macrophages were washed with PBS to remove extracellular *E. coli* and lysed with 100 μl of 0.1% sodium deoxycholate. The number of surviving bacteria was counted by plating on LB agar plates. Bacterial growth was also read continuously in a Fluostar fluorescence 96-well plate reader following the addition of 50 μl macrophage lysate to LB medium containing 10% (v/v) Alamar Blue.

**Statistical Analysis**

Data in figures are represented as mean ± SEM. Where indicated, p-values were calculated using either Student's t-test, a two-way ANOVA or repeated measures ANOVA with Dunnett's post-test statistic.

**ACCESSION NUMBER**

The microarray data reported in this paper have been submitted in MIAME compliant format at the Gene Expression Omnibus database (accession number GSE24524).

## Supplementary Text

### Mass spectrometric analysis of SNO-OxyR

In a first strategy (see Supplementary Materials and Methods), purified and S-nitrosylated OxyR (SNO-OxyR) was characterized by SNO-RAC modified by omission of thiol blocking prior to ascorbate treatment (*32*), followed by trypsin digest and mass spectrometry. Relative abundances of the cysteine-containing peptides based on the chromatographic peak area of peptide ions were compared in the presence or absence of ascorbate (Fig. S8). The normalized ratio (without ascorbate versus with ascorbate) for the Cys199-containing peptide was 0.13 ± 0.10 whereas the ratio for all other Cys-containing peptides was 1.0 ± 0.3 (n=2). That is, only the Cys199-containing peptide was enriched in an ascorbate-dependent manner (Figs. S8, S9), demonstrating that Cys199 was the sole site of S-nitrosylation and that all other Cys-containing peptides remained as free thiols.

In an alternative method (see Supplementary Materials and Methods), free thiols in SNO-OxyR were blocked with N-ethylmaleimide (NEM) followed by ascorbate-dependent carbamidomethylation with iodoacetamide (IAA). Cys199 was completely labeled with IAA in the presence of ascorbate (Fig. S10), confirming that it was S-nitrosylated. All other cysteines were NEM-labeled (Cys25 is shown as an example, Fig. S11), confirming that they were free thiols. A small percentage (<20%) of Cys25-peptide was also IAA labeled (n=1), which may account for the marginal increase over 1 SNO/mol OxyR in SNO-OxyR that we have detected, but just as likely represents incomplete blocking with NEM, as S-nitrosylation of Cys25 was not observed by SNO-RAC-based characterization (above). No disulfides or other oxidized forms of cysteine were detected.

**Supplementary Figures**

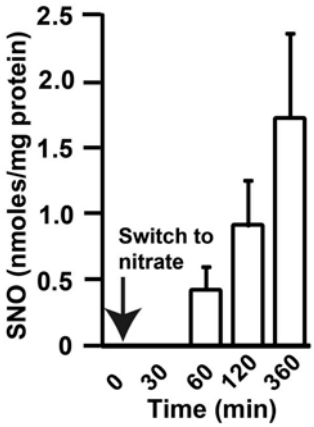


**Figure S1 Accumulation of S-nitrosothiols (SNO) during anaerobic growth on nitrate.** *E. coli* growing on 10 mM fumarate were switched at A600 of 0.3 to medium containing 10 mM nitrate. At the time points indicated, SNO levels in cell lysates were analyzed by Hg-coupled photolysis/chemiluminescence (n=3, ± SEM).

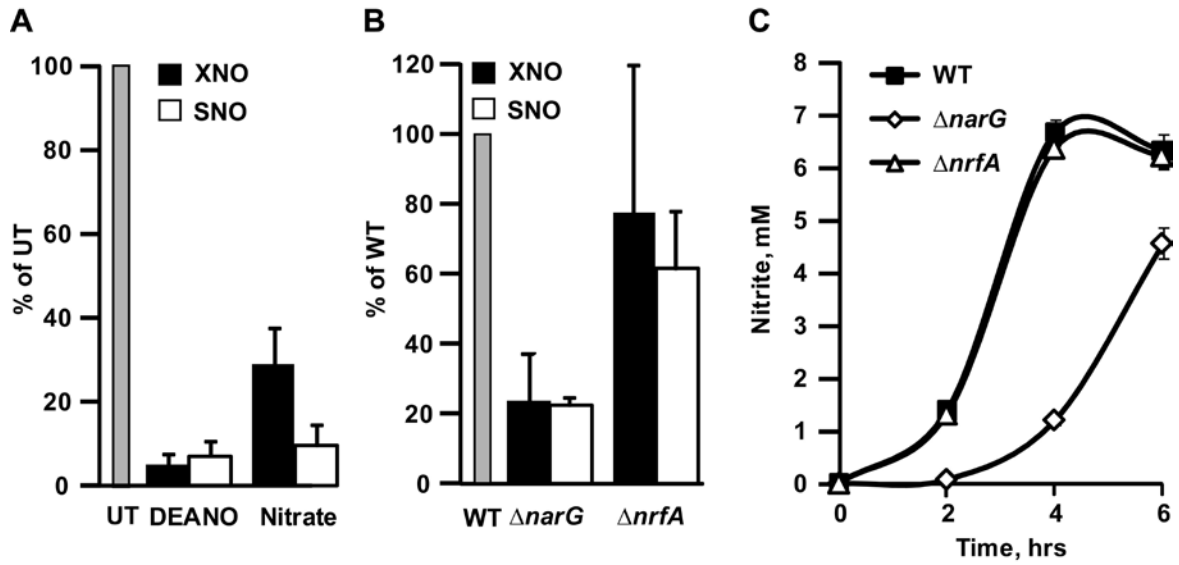


**Figure S2 (A) Transition metals contribute to anaerobic S-nitrosylation.** WT *E. coli* were grown anaerobically in minimal media and incubated with 1,10-phenanthroline (Phen) (1mM, 30 min) before treatment with either DEANO (100 μM, 30 min) or nitrate (10mM, 2 hrs). Lysates were analyzed by mercury-coupled photolysis/chemiluminescence: displacement of NO by mercury identifies SNO; XNO represents mercury–stable NO (n=3, ± SEM). UT, untreated

**(B) Nitrate reductase activity is required for optimal S-nitrosylation during anaerobic growth on nitrate.** WT, Δ*narG*, and Δ*nrfA E. coli* were grown on minimal medium with 10 mM nitrate and the lysates were analyzed by mercury-coupled photolysis/chemiluminescence (n=3, ± SEM). WT, wild type

**(C) Accumulation of nitrite in culture during growth on nitrate.** Nitrite levels in the cultures from (B) were analyzed by Greiss assay.

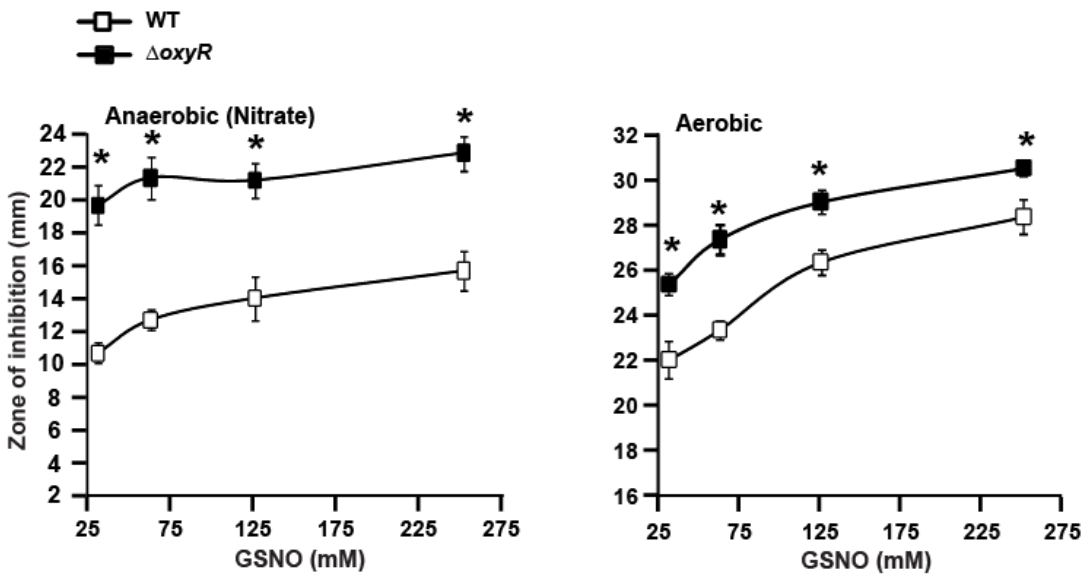


**Figure S3 OxyR protects against nitrosative stress.** Sensitivity of WT and *ΔoxyR* cells to different concentrations of GSNO was assessed in zone-of-inhibition assays. Data represent the diameter of the zone of inhibition by GSNO under aerobic or anaerobic conditions (n=3, ± SEM; * $p<0.05$). Note that the zone of inhibition by GSNO is substantially smaller under anaerobic (left panel) than aerobic (right panel) conditions.

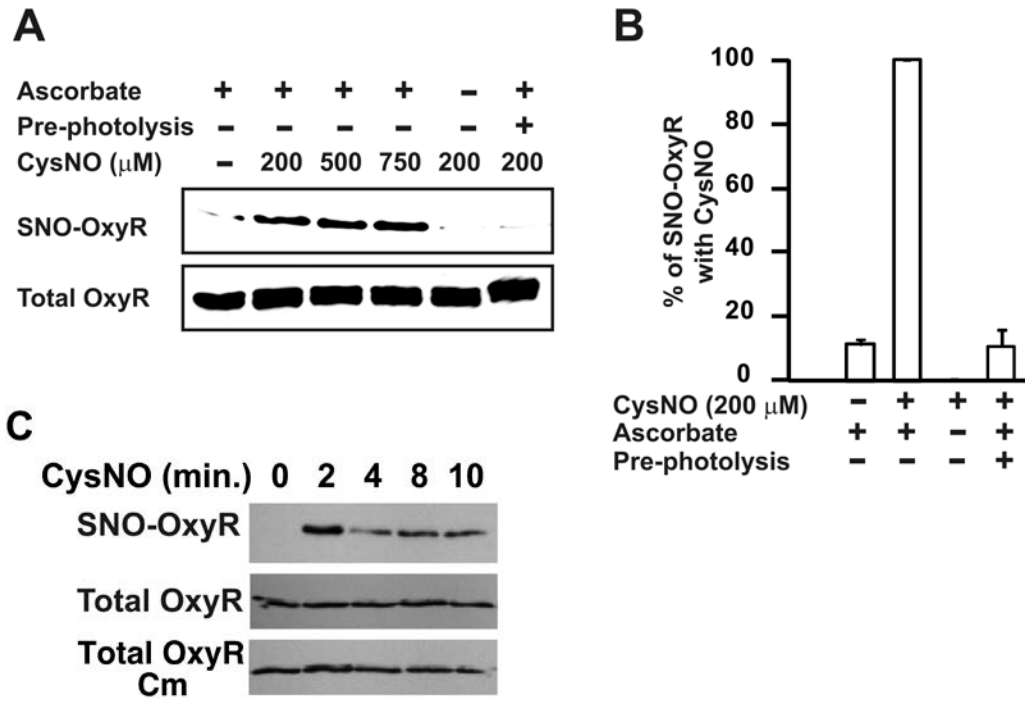


**Figure S4 (A) OxyR is *S*-nitrosylated under nitrosative stress.** *ΔoxyR*/OxyR-FLAG *E. coli* were grown anaerobically in minimal media containing 10 mM fumarate until A600 of 0.4 and then treated with the indicated concentrations of CysNO for 2 min. Lysates were subjected to SNO-RAC and OxyR was detected by Western blotting using anti-FLAG antibody. Omission of ascorbate or UV-photolysis prior to SNO-RAC served as controls.

**(B)** Densitometric analysis of the data in A (n=3, ± SEM).

**(C) Stability of OxyR is not influenced by S-nitrosylation.** *ΔoxyR/*OxyR-FLAG *E. coli* were grown anaerobically on 10 mM fumarate in minimal media until A600 of 0.4 and then treated with a single addition of CysNO (200 μM) for the indicated times. Cm indicates the addition of 100 μg/ml of the protein synthesis inhibitor chloramphenicol for 45 min prior to the addition of CysNO. Lysates were analyzed by SNO-RAC. The result is representative of three experiments. The time-dependent decrease in SNO-OxyR is not accompanied by changes in OxyR abundance (Total OxyR), indicating that it results from OxyR denitrosylation without a contribution from potential enhancement of SNO-OxyR degradation. In addition, OxyR abundance in the presence of CysNO is unaffected by pre-incubation with chloramphenicol (Total OxyR Cm).

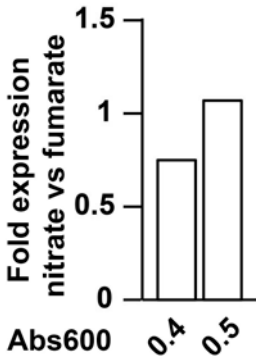


**Figure S5 Relative expression of oxyR during anaerobic growth.** *E. coli* were grown anaerobically on nitrate or fumarate (10 mM). The cells were harvested at A600 0.4 and 0.5. The expression levels of *oxyR* were determined by qPCR (n=2). Note that *E. coli* samples for microarray analysis (Figs. 2 and S6) were harvested at A600 0.4-0.45.

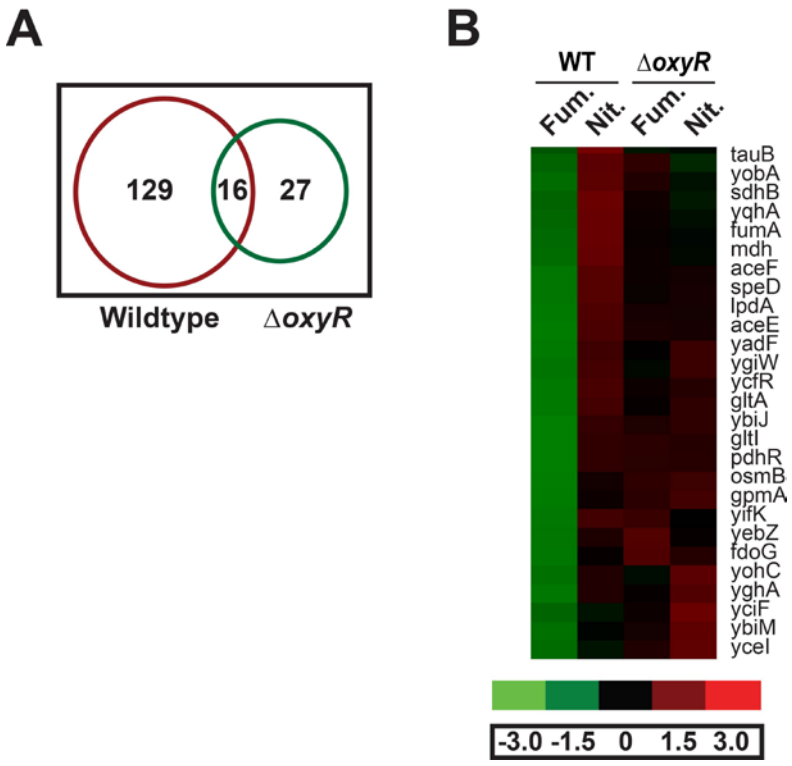


**Figure S6 (A) Venn diagram depicting the distribution of genes induced on nitrate.** The majority (n=129) of all genes (n=145) induced >2.0 fold during anaerobic growth on nitrate are OxyR-dependent. 16 genes showed induction by nitrate in both WT and *ΔoxyR* strains and 27 were induced by nitrate in *ΔoxyR* but not in WT.

**(B) Microarray analysis of gene induction in *E. coli* growing anaerobically.** Among the set of genes induced > two-fold in WT *E. coli* on nitrate versus fumarate (see Figure 2A for complete set), a relatively small subset, shown here, are more highly expressed on fumarate in *ΔoxyR* versus WT cells. GenspringGX software (Agilent) was used to analyze microarray results and genes were clustered using dChip.

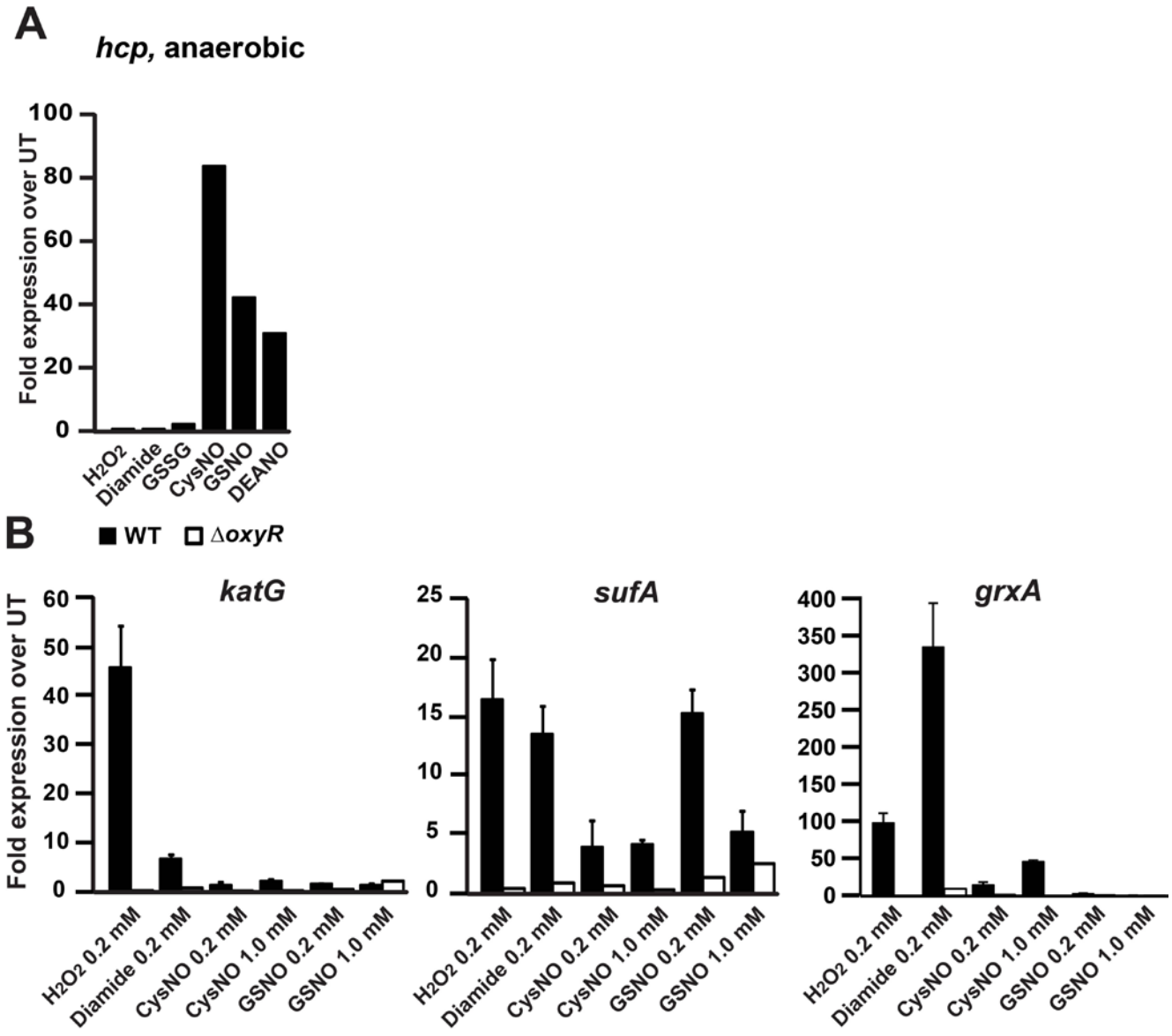


**Figure S7 (A) Potent upregulation of *hcp* by inducers of nitrosative but not oxidative stress**. *E. coli* grown anaerobically to A600 of 0.4 were treated with 200 μM of indicated reagents for 5 min before harvesting. The expression levels of *hcp* were determined by qPCR (n=2). UT = untreated.

**(B) Differential induction of OxyR-dependent genes by oxidative versus nitrosative stress**. *E. coli* were grown anaerobically to A600 of 0.4. The cells were treated with indicated reagents for 5 min before harvesting. The expression levels of *katG*, *sufA* and *grxA* were determined by qPCR (WT n=3, ± SEM; Δ*oxyR* n=2). UT = untreated. Note that induction was below the level of detection in many Δ*oxyR* samples.

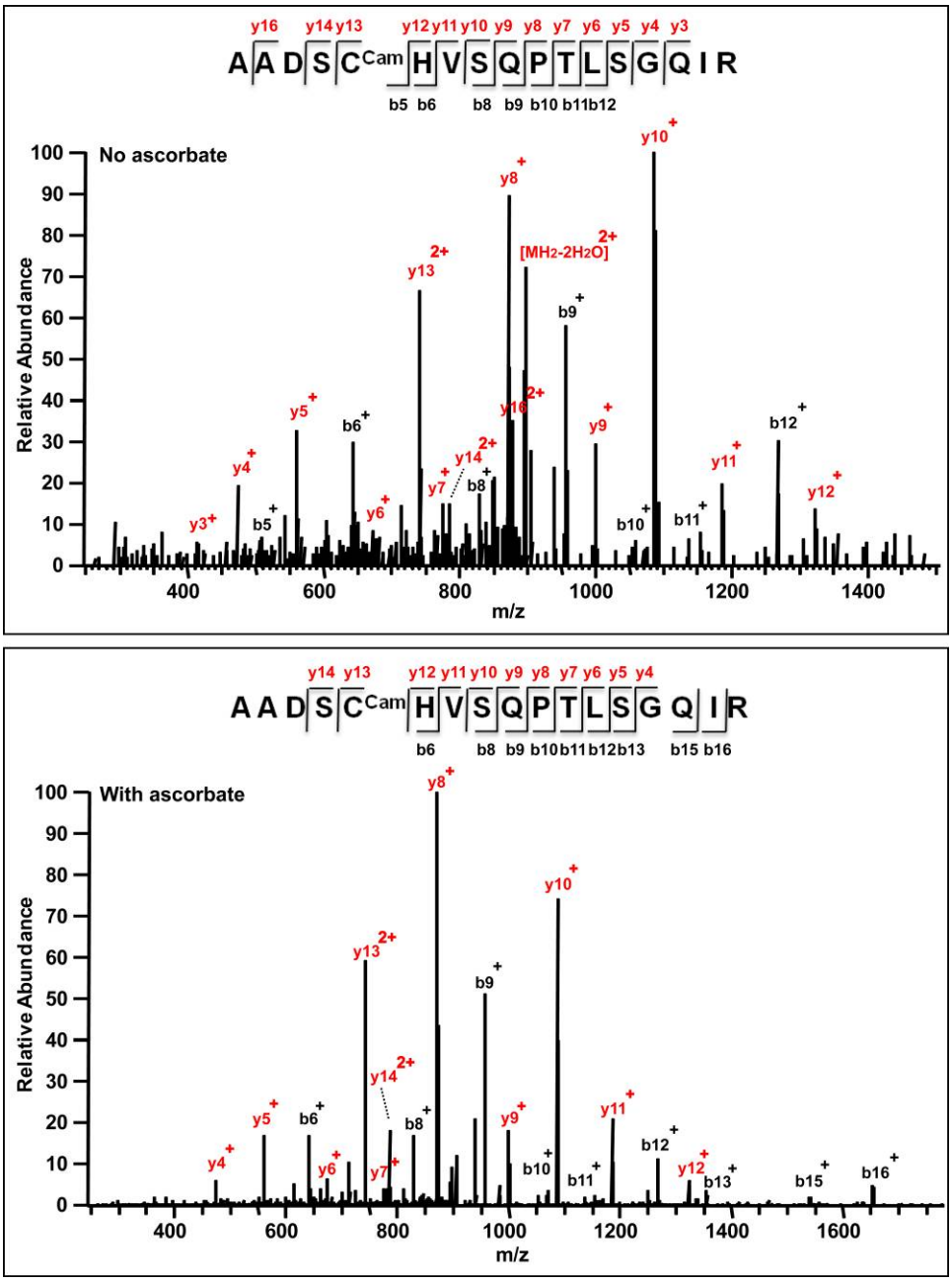


**Figure S8A MS/MS spectra of the cysteine-containing peptides in SNO-OxyR identified after SNO-RAC enrichment and LC-MS/MS analysis**. Shown are representative annotated MS/MS fragmentation spectra for the Cys25-containing peptide without ascorbate treatment (upper panel), and with ascorbate (lower panel) (See Supplementary Text). Peptide sequence is shown at the top of each spectrum, with the annotation of the identified matched amino terminus-containing ions (*b* ions) in black and the carboxyl terminus-containing ions (*y* ions) in red. For clarity, only major identified peaks are labeled.

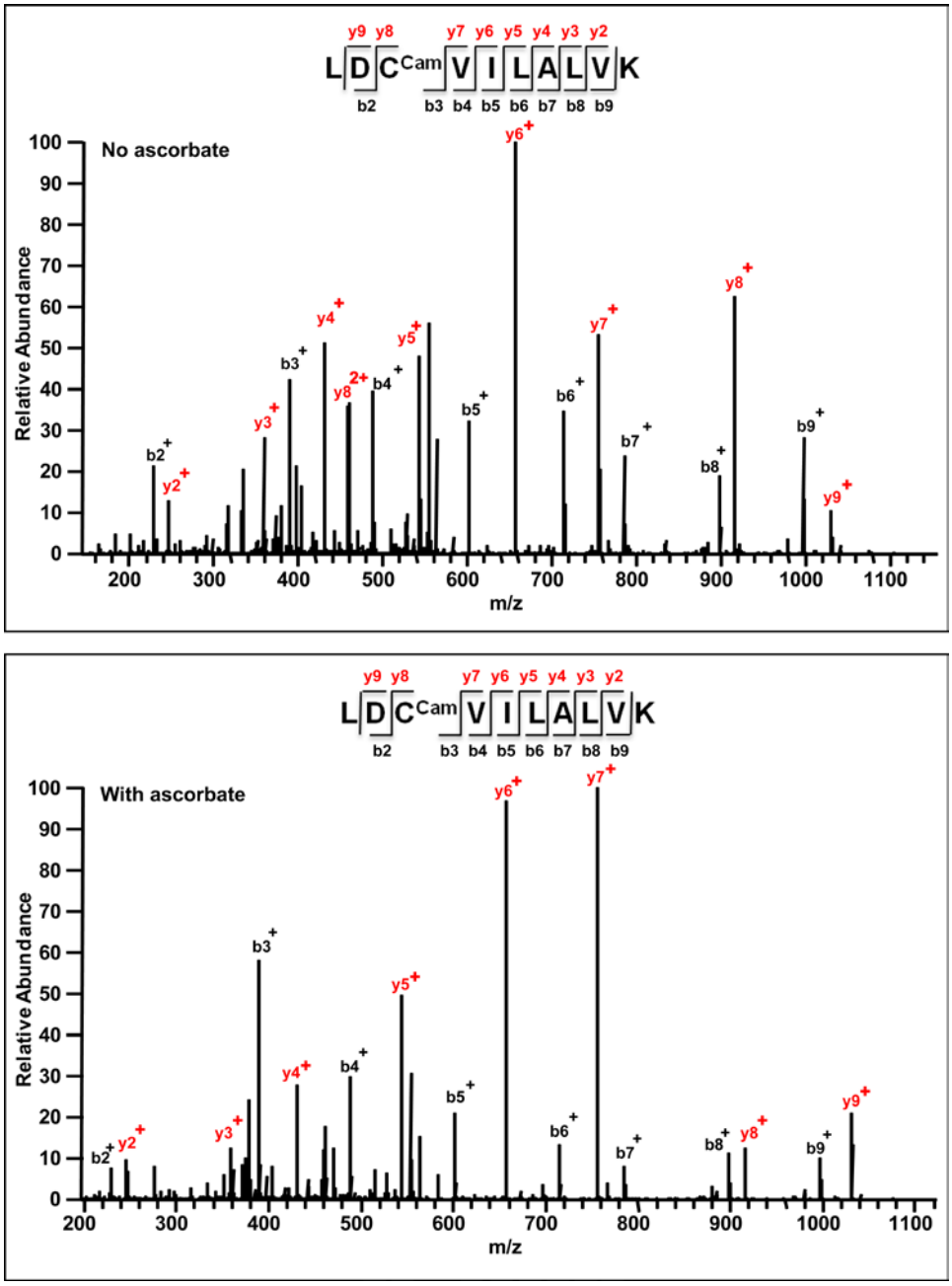


**Figure S8B MS/MS spectra of the cysteine-containing peptides in SNO-OxyR identified after SNO-RAC enrichment and LC-MS/MS analysis**. Shown are representative annotated MS/MS fragmentation spectra for the Cys143-containing peptide without ascorbate (upper panel), and with ascorbate (lower panel) (See Supplementary Text). Peptide sequence is shown at the top of each spectrum, with the annotation of the identified matched amino terminus-containing ions (*b* ions) in black and the carboxyl terminus-containing ions (*y* ions) in red. For clarity, only major identified peaks are labeled.

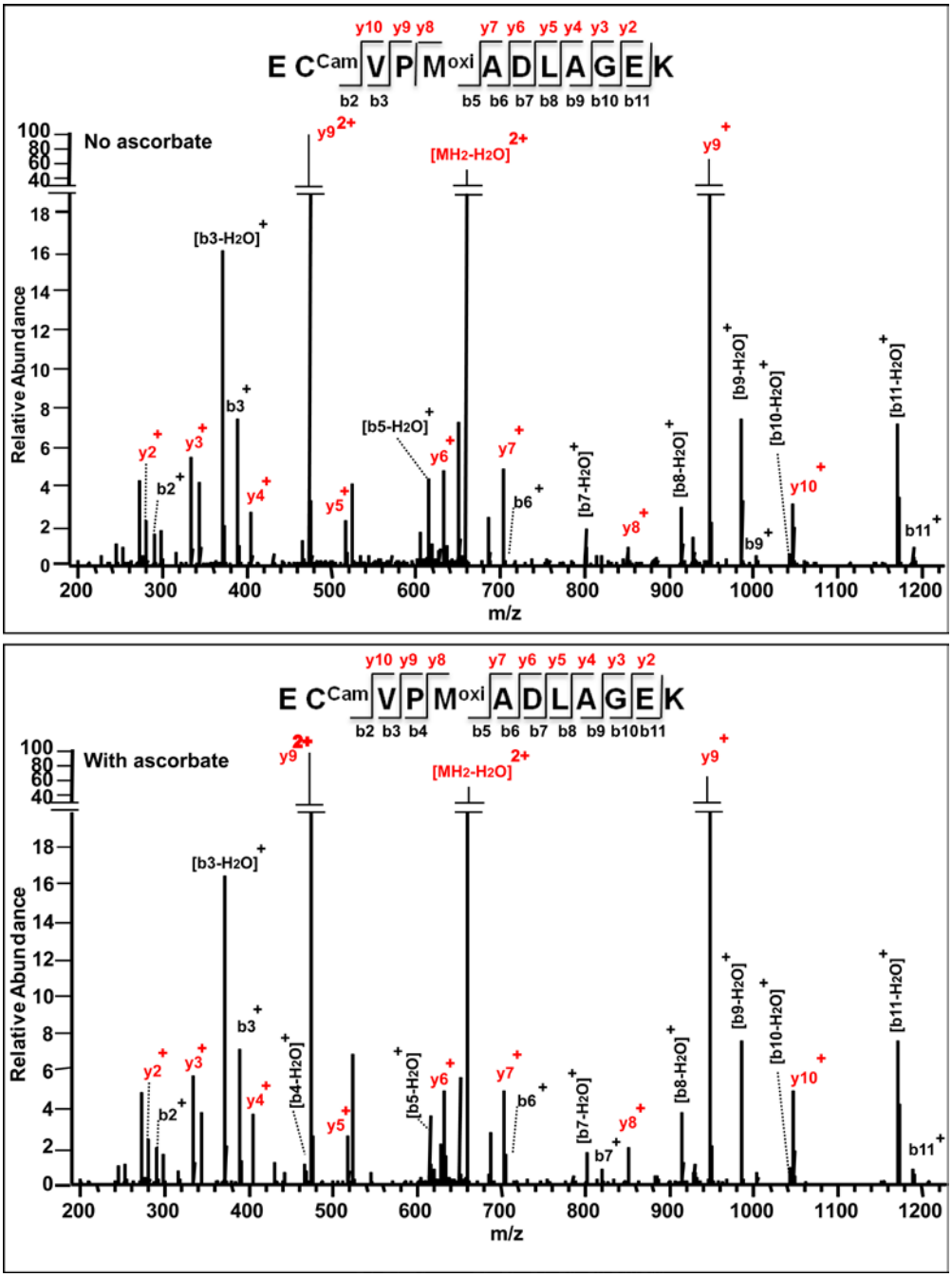


**Figure S8C MS/MS spectra of the cysteine-containing peptides in SNO-OxyR identified after SNO-RAC enrichment and LC-MS/MS analysis**. Shown are representative annotated MS/MS fragmentation spectra for the Cys180-containing peptide without ascorbate (upper panel), and with ascorbate (lower panel) (See Supplementary Text). Peptide sequence is shown at the top of each spectrum, with the annotation of the identified matched amino terminus-containing ions (*b* ions) in black and the carboxyl terminus-containing ions (*y* ions) in red. For clarity, only major identified peaks are labeled.

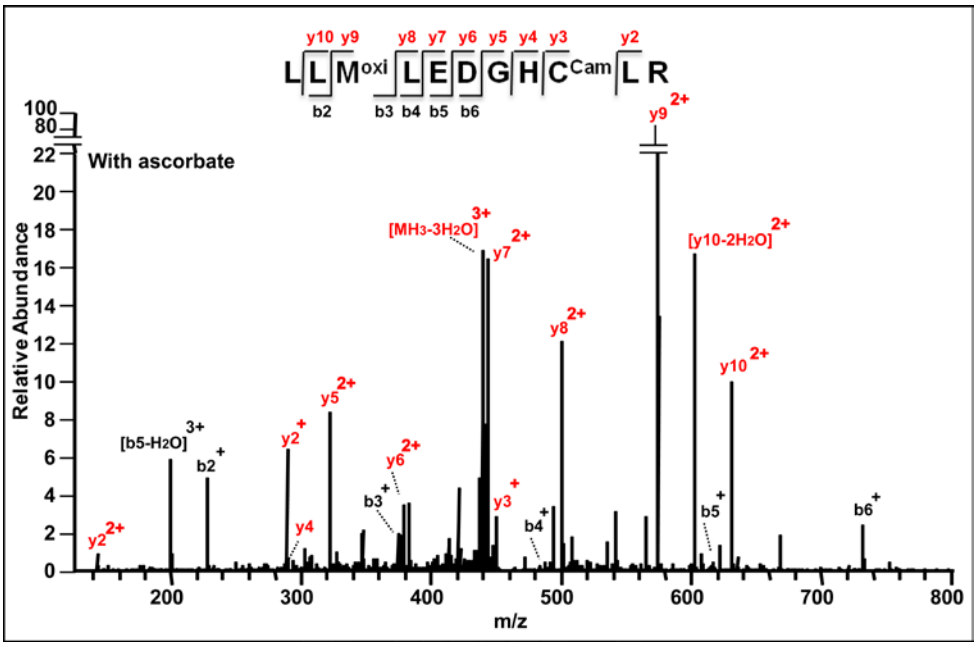


**Figure S8D MS/MS spectra of the cysteine-containing peptides in SNO-OxyR identified after SNO-RAC enrichment and LC-MS/MS analysis**. Shown are representative annotated MS/MS fragmentation spectra for the Cys199-containing peptide with ascorbate (See Supplementary Text). Cys199-containing peptide was not observed in the absence of ascorbate. Peptide sequence is shown at the top of each spectrum, with the annotation of the identified matched amino terminus-containing ions (*b* ions) in black and the carboxyl terminus-containing ions (*y* ions) in red. For clarity, only major identified peaks are labeled.

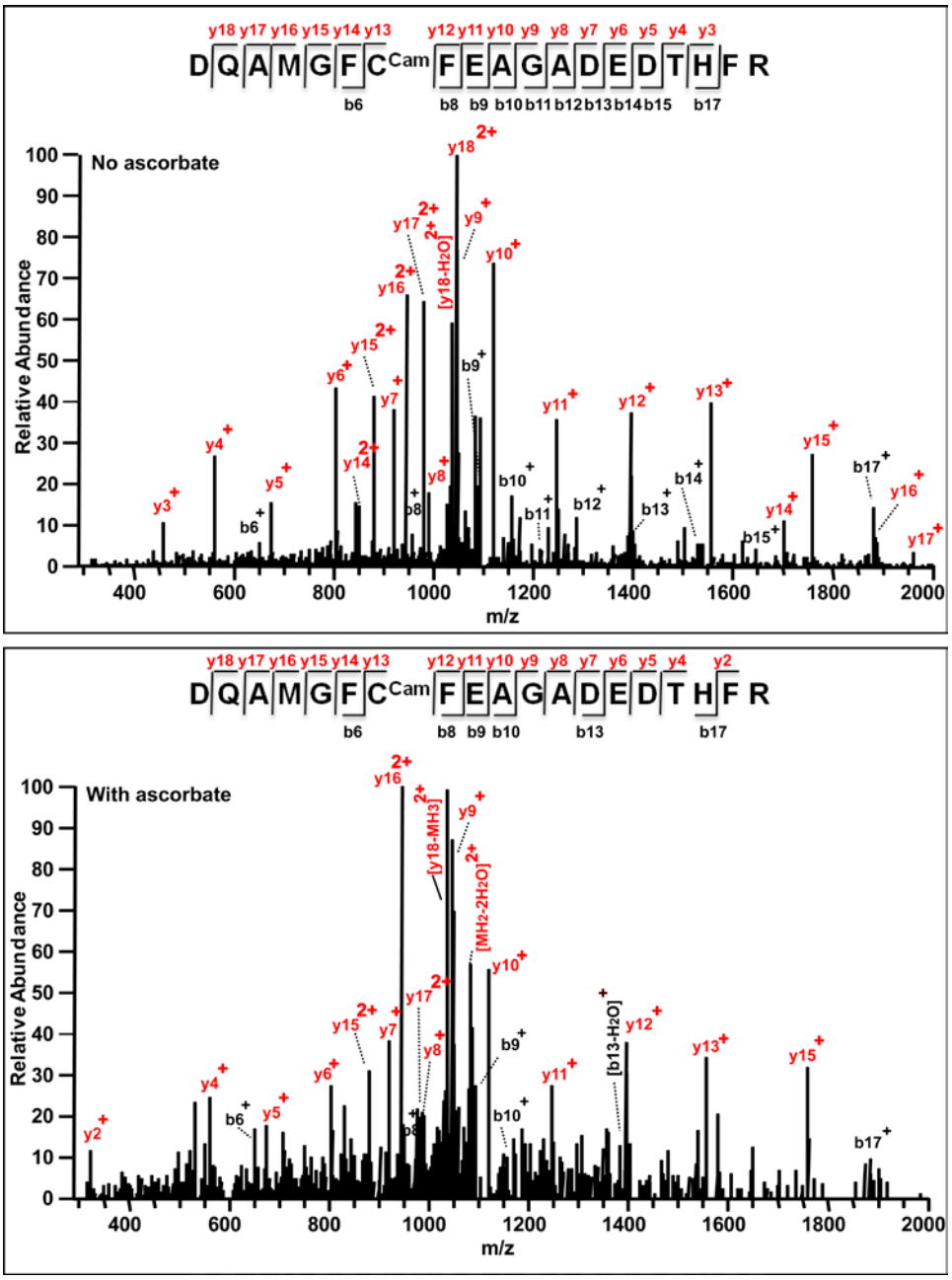


**Figure S8E MS/MS spectra of the cysteine-containing peptides in SNO-OxyR identified after SNO-RAC enrichment and LC-MS/MS analysis**. Shown are representative annotated MS/MS fragmentation spectra for the Cys208-containing peptide without ascorbate (upper panel), and with ascorbate (lower panel) (See Supplementary Text). Peptide sequence is shown at the top of each spectrum, with the annotation of the identified matched amino terminus-containing ions (*b* ions) in black and the carboxyl terminus-containing ions (*y* ions) in red. For clarity, only major identified peaks are labeled.

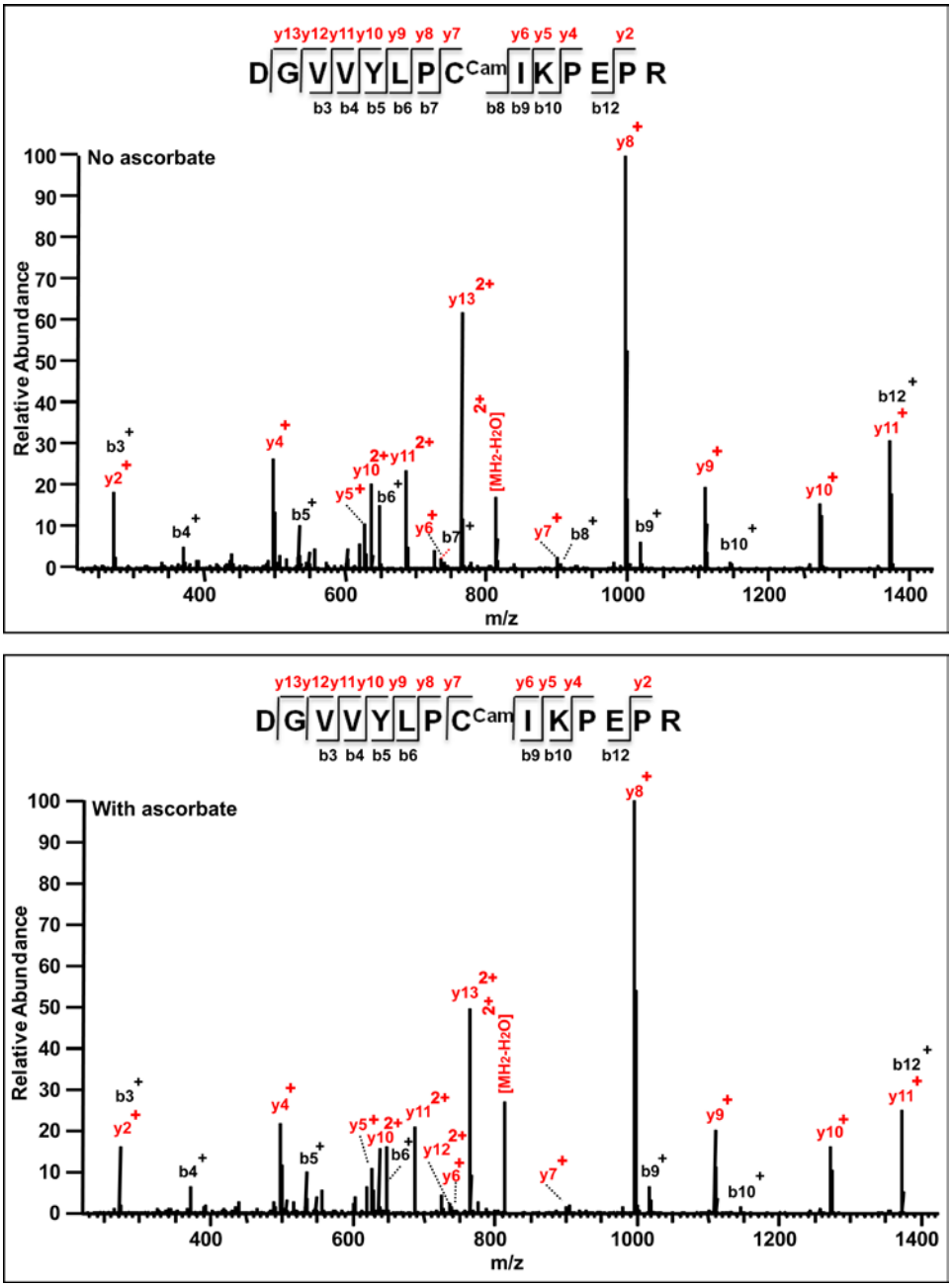


**Figure S8F MS/MS spectra of the cysteine-containing peptides in SNO-OxyR identified after SNO-RAC enrichment and LC-MS/MS analysis**. Shown are representative annotated MS/MS fragmentation spectra for the Cys259-containing peptide without ascorbate (upper panel), and with ascorbate (lower panel) (See Supplementary Text). Peptide sequence is shown at the top of each spectrum, with the annotation of the identified matched amino terminus-containing ions (*b* ions) in black and the carboxyl terminus-containing ions (*y* ions) in red. For clarity, only major identified peaks are labeled.

Peptides identified after modified SNO-RAC enrichment and tandem mass spectrometry.

| | Peptide sequence * | Cys | Precursor mass | Charge state | Δ mass (ppm) |
|---|---|---|---|---|---|
| -Asc | 21AADSC(Cam)HVSQPTLSGQIR37 | 25 | 913.9432 | 2 | -1.2 |
| | 141LDC(Cam)VILALVK150 | 143 | 572.3467 | 2 | 4.8 |
| | 179EC(Cam)VPM(Oxi)ADLAGEK190 | 180 | 668.3010 | 2 | 2.2 |
| | 202DQAMGFC(Cam)FEAGADEDTHFR220 | 208 | 1102.4399 | 2 | -3.7 |
| | 252DGVVYLPC(Cam)IKPEPR265 | 259 | 821.9357 | 2 | 1.2 |
| +Asc | 21AADSC(Cam)HVSQPTLSGQIR37 | 25 | 913.9456 | 2 | 1.4 |
| | 141LDC(Cam)VILALVK150 | 143 | 572.3470 | 2 | 5.3 |
| | 179EC(Cam)VPM(Oxi)ADLAGEK190 | 180 | 668.2986 | 2 | -1.5 |
| | 191LLM(Oxi)LEDGHC(Cam)LR201 | 199 | 458.2271 | 3 | -3.2 |
| | 202DQAMGFC(Cam)FEAGADEDTHFR220 | 208 | 1102.4399 | 2 | -3.7 |
| | 252DGVVYLPC(Cam)IKPEPR265 | 259 | 821.9364 | 2 | 2.1 |

**Figure S9 Specific S-nitrosylation of Cys199 in SNO-OxyR.** SNO-OxyR prepared *in vitro* was subjected to modified SNO-RAC and enriched peptides were identified by LC-MS/MS (see Supplementary Materials and Methods and Supplementary Text). Peptides containing Cys199 were identified only after ascorbate treatment, which removes the NO group from S-nitrosylated Cys residues. * (Cam) and (Oxi) indicate cysteine carbamidomethylation and methionine oxidation respectively.

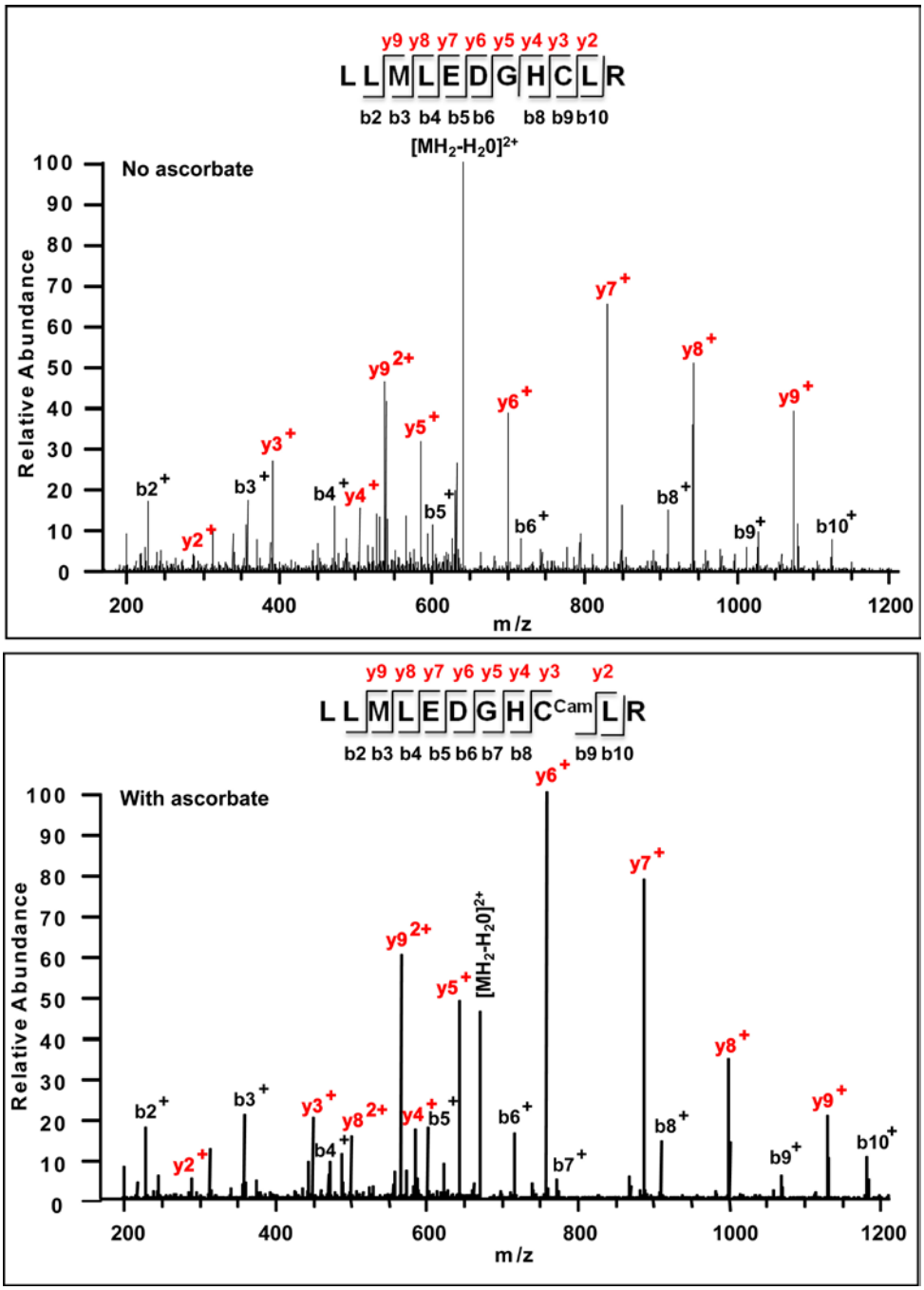


**Figure S10 Ascorbate-dependent cysteine alkylation of Cys199 detected by LC-MS/MS (strategy employing NEM treatment and ascorbate-dependent IAA labeling).** Shown are representative annotated MS/MS fragmentation spectra for the Cys199-containing doubly charged peptide LLMLEDGHCLR without ascorbate (upper panel), and LLMLEDGHC$^{(carbamidomethyl)}$LR with ascorbate (lower panel) (See Supplementary Text). Peptide sequence is shown at the top of each spectrum, with the annotation of the identified matched amino terminus-containing ions (*b* ions) in black and the carboxyl terminus-containing ions (*y* ions) in red. For clarity, only major identified peaks are labeled.

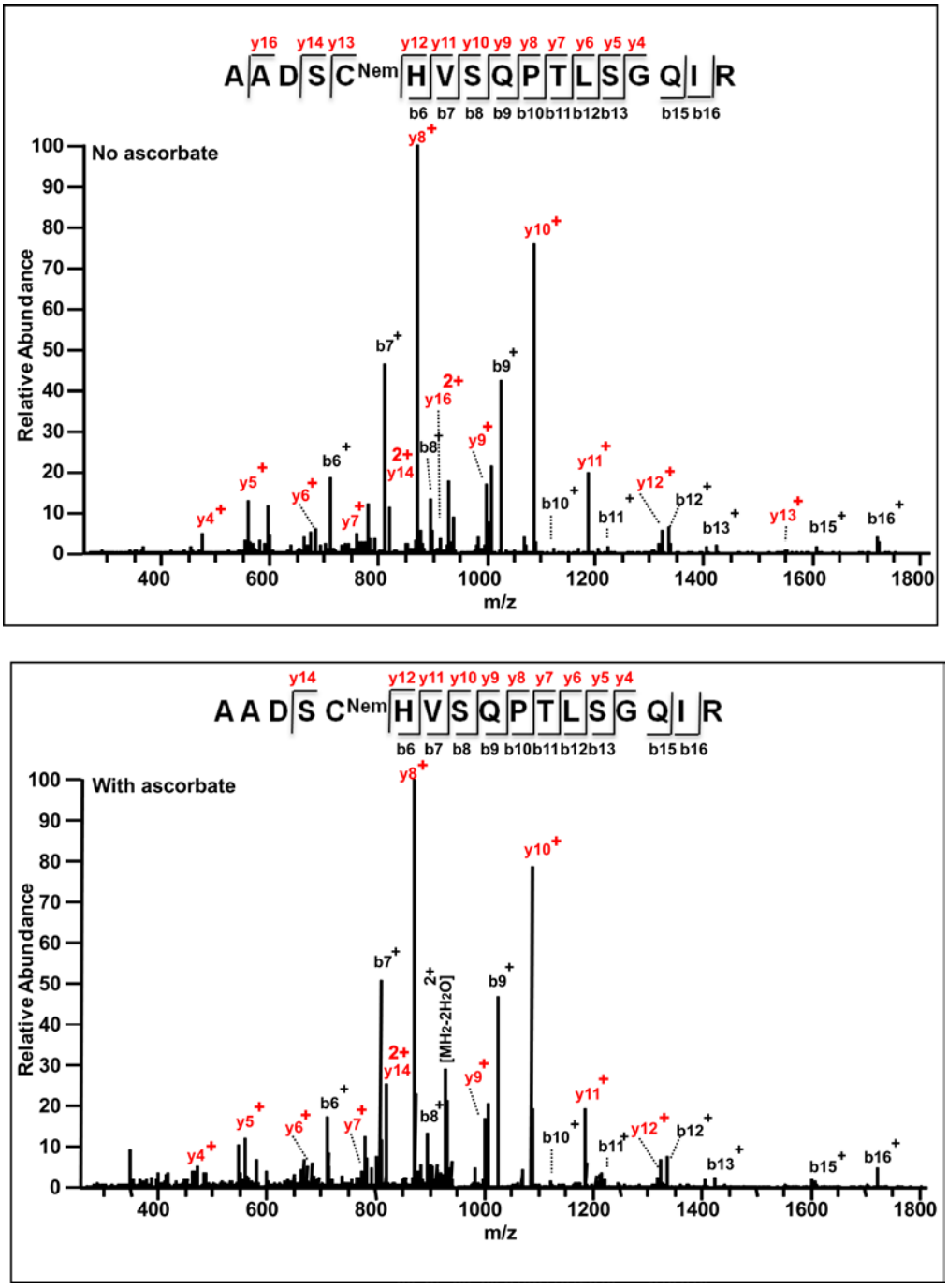


**Figure S11 Ascorbate-dependent cysteine alkylation of Cys25 detected by LC-MS/MS (strategy employing NEM treatment and ascorbate-dependent IAA labeling).** Shown are representative annotated MS/MS fragmentation spectra for the Cys25-containing peptide AADSC$^{(Nem)}$HVSQPTLSGQIR without ascorbate (upper panel), and AADSC$^{(Nem)}$HVSQPTLSGQIR with ascorbate (lower panel) (See Supplementary Text). Peptide sequence is shown at the top of each spectrum, with the annotation of the identified matched amino terminus-containing ions (*b* ions) in black and the carboxyl terminus-containing ions (*y* ions) in red. For clarity, only major identified peaks are labeled.

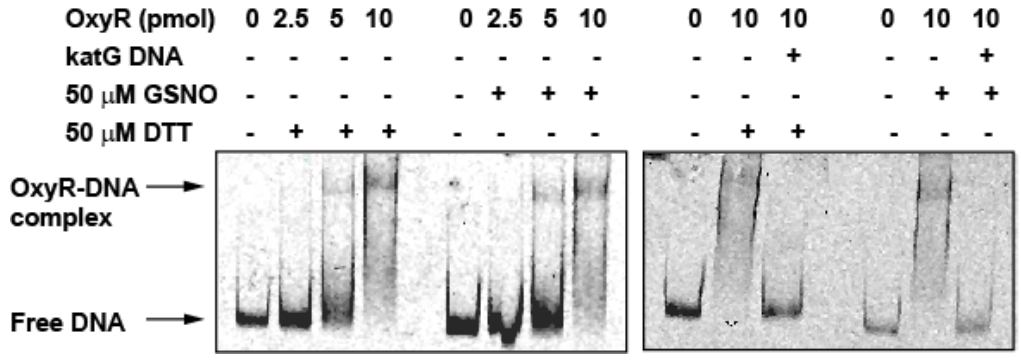


**Figure S12 Electrophoretic mobility shift assay shows that the *hcp* promoter includes a specific OxyR binding site.** Increasing amounts of OxyR were incubated with *hcp* promoter DNA. Binding was decreased competitively by unlabeled *katG* promoter DNA that included the OxyR-binding site. IR-800 dye-labeled DNA bands were separated on 5% polyacrylamide gels and visualized with an Odyssey imaging system (LICOR).

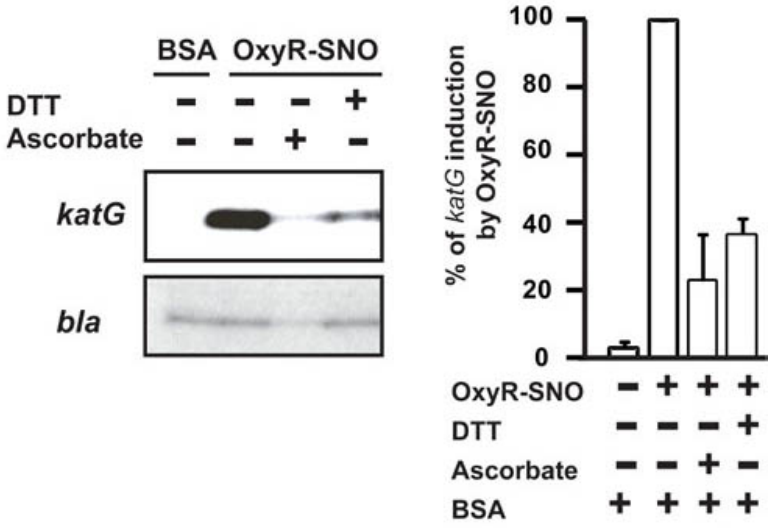


**Figure S13 *In vitro* transcription at *katG* promoter by S-nitrosylated OxyR.** Primer extension products of *in vitro* transcription reactions with S-nitrosylated OxyR are shown. Plasmid containing the *katG* gene (along with the β-lactamase (*bla*) gene) was used as template. DTT and ascorbate were used at 100 mM. Right panel shows quantification of primer extension bands for *katG*. Results are expressed as % induction by OxyR-SNO, normalized with respect to *bla* control (n=3 separate OxyR-SNO preparations, ± SEM).

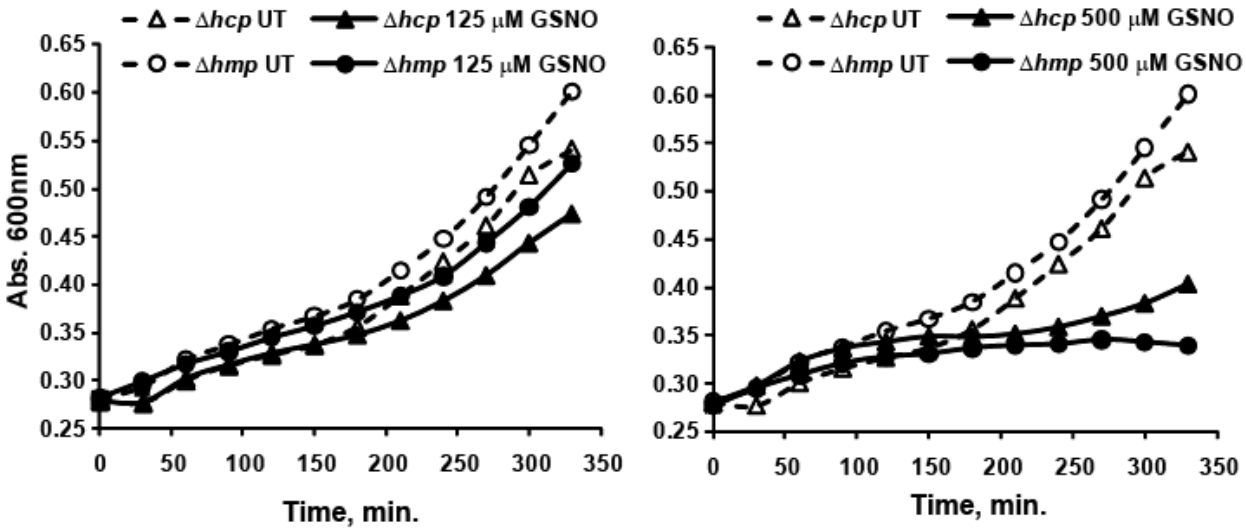


**Figure S14 Sensitivity of *Δhcp* mutant to GSNO is comparable to that of *Δhmp in vitro*.** Growth of *Δhcp* and *Δhmp E. coli* was measured following treatment with increasing concentrations of GSNO (125-500μM). Time 0 indicates initiation of treatment (n=3). UT= untreated.

**Table S1. Genes expressed > 3-fold during anaerobic respiration on nitrate in WT *E. coli***

| Protein function (Gene name) | Gene | Fold change WT | Fold change Δ*oxyR* | Protein function (Gene name) | Gene | Fold change WT | Fold change Δ*oxyR* |
|---|---|---|---|---|---|---|---|
| 3-isopropylmalate dehydrogenase **leuB** | b0073 | **3.45** | **0.54** | Hypothetical protein **yciW** | b1287 | **4.69** | **0.90** |
| Pyruvate dehydrogenase complex repressor **pdhR** | b0113 | **4.10** | **1.01** | Methylated-DNA-protein-cysteine methyltransferase ogt | b1335 | 7.71 | 6.57 |
| Dihydrolipoamide dehydrogenase **lpdA** | b0116 | **3.06** | **0.98** | Tellurite resistance protein tehA | b1429 | 5.26 | 5.16 |
| Aconitate hydrase B **acnB** | b0118 | **3.51** | **0.99** | Tellurite resistance protein tehB | b1430 | 3.76 | 3.59 |
| Glucose dehydrogenase **gcd** | b0124 | **3.63** | **1.13** | Formate dehydrogenase **fdnG** | b1474 | **48.14** | **1.34** |
| Taurine-binding periplasmic protein **tauA** | b0365 | **8.14** | **1.18** | Formate dehydrogenase-N **fdnH** | b1475 | **17.99** | **0.97** |
| Taurine transport protein **tauB** | b0366 | **5.26** | **0.85** | Formate dehydrogenase-N **fdnI** | b1476 | **7.42** | **1.14** |
| Protoheme farnesyltransferase **cyoE** | b0428 | **3.27** | **1.13** | Hypothetical protein **yeaC** | b1777 | **6.27** | **0.80** |
| Cytochrome O ubiquinol oxidase **cyoD** | b0429 | **6.88** | **0.97** | Methionine sulfoxide reductase **msrB** | b1778 | **8.25** | **0.86** |
| Cytochrome O ubiquinol oxidase **cyoC** | b0430 | **3.45** | **0.90** | Hypothetical protein yoaG | b1796 | 104.4 | 54.24 |
| Ubiquinol oxidase polypeptide I **cyoB** | b0431 | **3.59** | **0.94** | Tellurite resistance protein yeaR | b1797 | 172.4 | 21.63 |
| Hypothetical protein **ybaY** | b0453 | **3.62** | **1.23** | Hypothetical protein yedU | b1967 | 4.91 | 2.44 |
| Hypothetical protein **ylaC** | b0458 | **3.54** | **0.87** | Transcriptional regulator **cbl** | b1987 | **3.09** | **1.20** |
| Citrate synthase **gltA** | b0720 | **3.25** | **1.21** | Flavohemoprotein hmpA | b2552 | 23.91 | 20.62 |
| Phosphoglycerate mutase 1 **gpmA** | b0755 | **3.27** | **1.10** | Hypothetical protein **yfiM** | b2586 | **5.16** | **1.03** |
| Hypothetical oxidoreductase **ybiC** | b0801 | **5.67** | **0.99** | Alpha-ketoglutarate permease **kgtP** | b2587 | **5.57** | **1.02** |
| Hypothetical protein **ybiJ** | b0802 | **3.86** | **1.10** | RNA polymerase, sigma S factor **rpoS** | b2741 | **4.63** | **1.15** |
| Hypothetical protein yliH | b0836 | 3.92 | 1.94 | Sulfite reductase [NADPH] hemoprotein beta-component**cysI** | b2763 | **4.68** | **1.03** |
| NADH oxidoreductase **hcr** | b0872 | **15.62** | **3.04** | Hypothetical protein **yqhA** | b3002 | **3.41** | **0.83** |
| Hybrid cluster protein **hcp** | b0873 | **38.38** | **5.55** | Cold-shock DEAD-box protein A **deaD** | b3162 | **3.54** | **1.05** |
| FMN reductase **ssuE** | b0937 | **4.08** | **1.12** | Thiosulfate sulfurtransferase **glpE** | b3425 | **3.66** | **0.99** |
| Exopolysaccharide production yccZ | b0983 | 3.42 | 2.29 | Hypothetical protein **yzgL** | b3427 | **3.57** | **0.73** |
| Hypothetical protein ymcB | b0985 | 4.45 | 2.66 | Threonine 3-dehydrogenase tdh | b3616 | 3.14 | 1.49 |
| Hypothetical protein ycfJ | b1110 | 3.07 | 1.90 | Acetolactate synthase isozyme I **ilvN** | b3670 | **4.89** | **1.13** |
| Hypothetical protein **ycfR** | b1112 | **5.71** | **1.09** | Acetohydroxy acid synthase II **ilvG** | b3768 | **3.49** | **1.25** |
| Hypothetical protein **ycgZ** | b1164 | **10.14** | **1.31** | Dihydroxyacid dehydratase **ilvD** | b3771 | **4.84** | **0.98** |
| Unknown CDS **ymgA** | b1165 | **11.82** | **1.39** | Threonine deaminase **ilvA** | b3772 | **5.67** | **1.05** |
| Unknown CDS **ymgC** | b1167 | **8.74** | **0.96** | Formate dehydrogenase **fdoI** | b3892 | **3.94** | **1.50** |
| D-amino acid dehydrogenase**dadA** | b1189 | **6.39** | **0.89** | Formate dehydrogenase-O **fdoG** | b3894 | **8.85** | **0.77** |
| Alanine racemase **dadX** | b1190 | **5.21** | **0.95** | Isocitrate lyase **aceA** | b4015 | **3.74** | **0.71** |
| Nitrate reductase 1 narG | b1224 | 3.41 | 2.00 | Hypothetical protein **yjbA** | b4030 | **4.33** | **1.29** |
| Respiratory nitrate reductase 1 **narI** | b1227 | **3.31** | **1.16** | Fe-S cluster repair ytfE | b4209 | 67.25 | 19.52 |
| Aconitate hydratase 1 **acnA** | b1276 | **4.47** | **1.12** | Hypothetical protein ISO92 | b4434 | 3.04 | 1.25 |

**Table S1** Microarray data comparing fold-expression of genes in WT and Δ*oxyR E. coli* grown anaerobically on 10 mM nitrate or fumarate. Genes induced > 3-fold in the WT on nitrate are included (p-value cutoff of 0.05). The corresponding induction levels in Δ*oxyR* are given. Genes whose fold-induction on nitrate in Δ*oxyR* was at least two-fold lower than induction in WT, and which are thus potential OxyR-dependent genes, are indicated in bold. Genes are listed in the order of their b-number and have been arranged into operons (delineated by solid lines) via *E. coli* Entry Point.

**Table S2. Genes expressed between 2- and 3-fold during anaerobic respiration on nitrate in WT *E. coli***

| Protein function (Gene name) | Gene | Fold change WT | Fold change Δ*oxyR* | Protein function (Gene name) | Gene | Fold change WT | Fold change Δ*oxyR* |
|---|---|---|---|---|---|---|---|
| 3-isopropylmalate isomerase leuD | b0071 | 2.83 | 0.53 | Putative transport component yeeE | b2013 | 2.30 | 0.91 |
| Pyruvate dehydrogenase E1 component aceE | b0114 | 2.40 | 0.97 | Hypothetical protein yohL | b2105 | 2.30 | 1.23 |
| S-adenosylmethionine decarboxylase speD | b0120 | 2.09 | 1.03 | Hypothetical protein yohC | b2135 | 2.31 | 1.46 |
| Putative carbonic anhydrase yadF | b0126 | 2.01 | 1.16 | Trehalose-phosphatase otsB | b1897 | 2.43 | 1.29 |
| Putative phage integrase intF | b0281 | 2.37 | 0.96 | Cytochrome c-type protein napB | b2203 | 2.81 | 0.75 |
| Hypothetical protein ykgE | b0306 | 2.56 | 8.67 | Naphthoate synthase menB | b2262 | 2.09 | 1.98 |
| Cyanate aminohydrolase cynS | b0340 | 2.18 | 1.56 | NADH dehydrogenase I chain I nuoI | b2281 | 2.46 | 1.24 |
| ATP-dependent protease La lon | b0439 | 2.19 | 1.28 | Putative malic oxidoreductase maeB | b2463 | 2.17 | 0.89 |
| Chaperone protein htpG | b0473 | 2.16 | 1.34 | NifU-like protein iscU | b2529 | 2.11 | 2.53 |
| Hypothetical protein ylbA | b0515 | 2.07 | 0.87 | ATP-dependent protease clpB | b2592 | 2.56 | 1.66 |
| Lipoic acid synthetase lipA | b0628 | 2.52 | 0.93 | ATP:sulfate adenylyltransferase cysD | b2752 | 2.72 | 0.91 |
| Glutamate/aspartate periplasmic binding protein ybeJ | b0655 | 2.52 | 0.97 | Hypothetical lipoprotein ygdI | b2809 | 2.33 | 1.59 |
| Succinate dehydrogenase sdhB | b0724 | 2.02 | 1.00 | Glycine dehydrogenase gcvP | b2903 | 2.25 | 1.19 |
| Succinyl-CoA synthetase a chain sucD | b0729 | 2.13 | 0.89 | Hypothetical oxidoreductase yghA | b3003 | 2.95 | 1.51 |
| Molybdenum cofactor biosynthesis protein B moaB | b0782 | 2.29 | 1.52 | Hypothetical RNA polymerase, sigma(70) factor rpoD | b3067 | 2.65 | 1.08 |
| Hypothetical protein ybiM | b0806 | 2.06 | 1.23 | Malate dehydrogenase mdh | b3236 | 2.92 | 0.88 |
| Molybdopterin biosynthesis moeA | b0827 | 2.18 | 1.87 | Gluconate transporter; gntP | b3415 | 2.04 | 0.94 |
| ATP-dependent clp protease ATP-binding subunit clpA | b0882 | 2.30 | 1.06 | Glycerol-3-phosphate dehydrogenase (aerobic) glpD | b3426 | 2.88 | 1.24 |
| Putative electron transport protein yccM | b0992 | 2.40 | 1.28 | Hypothetical transporter yhiP | b3496 | 2.48 | 1.26 |
| Putative secreted protein yceI | b1056 | 2.15 | 1.08 | Hypothetical metabolite transport protein yhjE | b3523 | 2.52 | 1.09 |
| Glutamyl tRNA reductase hemA | b1210 | 2.04 | 1.61 | Glycine acetyltransferase kbl | b3617 | 2.15 | 1.35 |
| Putative structural proteins yciF | b1258 | 2.20 | 1.31 | Acetohydroxy acid synthase II ilvG | b3767 | 2.28 | 1.15 |
| Osmotically inducible lipoprotein B precursor osmB | b1283 | 2.20 | 1.03 | Acetolactate synthase isozyme II subunit ilvM | b3769 | 2.62 | 1.15 |
| Thiol peroxidase tpx | b1324 | 2.77 | 0.97 | Amino acid aminotransferase ilvE | b3770 | 2.26 | 0.90 |
| Hypothetical protein ynaJ | b1332 | 2.81 | 0.93 | Probable transport protein yifK | b3795 | 2.09 | 0.83 |
| Hypothetical protein ydcN | b1434 | 2.63 | 0.96 | Affects formate dehydrogenaseN;fdhE | b3891 | 2.18 | 1.41 |
| Fumarate hydratase class I fumA | b1612 | 2.37 | 0.85 | Glycerol uptake facilitator protein glpF | b3927 | 2.47 | 1.07 |
| Glutathione S-transferase gst | b1635 | 2.51 | 1.02 | Molecular chaperone hslU | b3931 | 2.39 | 1.11 |
| Hypothetical protein ynhG ; | b1678 | 2.71 | 1.21 | ATP-dependent protease hslV | b3932 | 2.21 | 1.16 |
| Spheroplast protein Y precursor spy | b1743 | 2.16 | 1.29 | Peroxidase/catalase HPI katG | b3942 | 2.28 | 1.07 |
| Hypothetical protein yeaQ | b1795 | 2.17 | 1.84 | Thiazole biosynthesis protein thiH | b3990 | 2.65 | 1.04 |
| L-serine dehydratase 1 sdaA | b1814 | 2.07 | 1.20 | Malate synthase A aceB | b4014 | 2.23 | 0.79 |
| Hypothetical protein yebZ | b1840 | 2.83 | 0.73 | Homocysteine-methyltetrahydrofolate transmethylase metH | b4019 | 2.33 | 1.05 |
| Hypothetical protein yobA | b1841 | 2.24 | 0.85 | Hypothetical protein yjcB | b4060 | 2.17 | 1.04 |
| Trehalose-6-phosphate synthase otsA | b1896 | 2.34 | 1.21 | Proline permease II proP | b4111 | 2.21 | 1.12 |
| Trehalose-phosphatase otsB | b1897 | 2.43 | 1.30 | Methionine sulfoxide reductase msrA | b4219 | 2.15 | 1.18 |
| Hypothetical protein yodD | b1953 | 2.14 | 1.47 | Ribonucleoside reductase nrdD | b4238 | 2.29 | 1.06 |
| Hypothetical protein yedP | b1955 | 2.13 | 1.30 | | | | |

**Table S2** Microarray data comparing fold-expression of genes during anaerobic growth of WT and Δ*oxyR E.coli* on 10 mM nitrate or fumarate. Genes induced between 2- and 3-fold on nitrate versus fumarate in the WT are included. The corresponding induction levels for Δ*oxyR* are given. Genes are listed in the order of their b-number and have been arranged into operons (delineated by solid lines) via *E. coli* Entry Point.

**Table S3. Genes expressed >2-fold during anaerobic respiration on nitrate in Δ*oxyR*.**

| Protein function (Gene name) | Gene | Fold change WT | Fold change Δ*oxyR* | Protein function (Gene name) | Gene | Fold change WT | Fold change Δ*oxyR* |
|---|---|---|---|---|---|---|---|
| Iron-sulfur cluster insertion protein erpA | b0156 | 1.18 | 2.43 | Hypothetical protein yoaG | b1796 | 104.24 | 68.1 |
| Uncharacterized protein ykgE | b0306 | 2.55 | 9.55 | Tellurite resistance protein yeaR | b1797 | 172.4 | 21.63 |
| Uncharacterized electron transport protein ykgF | b0307 | 1.76 | 9.04 | Hypothetical protein yedU | b1967 | 4.91 | 2.45 |
| Uncharacterized protein ykgG | b0308 | 1.18 | 7.09 | Membrane protein yohJ | b2141 | 0.25 | 2.63 |
| Uncharacterized protein ybhK | b0780 | 1.47 | 2.17 | Inner membrane protein yohK | b2142 | 0.32 | 2.38 |
| NADH oxidoreductase hcr | b0872 | 15.62 | 3.10 | Inner membrane protein yeiH | b2158 | 1.23 | 2.85 |
| Hybrid cluster protein hcp | b0873 | 38.38 | 5.56 | Co-chaperone protein hscB | b2527 | 1.73 | 2.35 |
| Exopolysaccharide production yccZ | b0983 | 3.42 | 2.28 | Iron-binding protein iscA | b2528 | 1.48 | 2.04 |
| Hypothetical protein ymcB | b0985 | 4.44 | 2.65 | Iron-sulfur cluster assembly enzyme iscU | b2529 | 2.11 | 2.53 |
| Respiratory nitrate reductase 1 alpha chain narG | b1224 | 3.4 | 2.00 | Cysteine desulfurase iscS | b2530 | 1.44 | 2.12 |
| Methylated-DNA-protein-cysteine methyltransferase ogt | b1335 | 7.71 | 6.68 | HTH-type transcriptional regulator iscR | b2531 | 1.82 | 2.36 |
| Tellurite resistance protein tehA | b1429 | 5.26 | 5.16 | Flavohemoprotein hmp | b2552 | 23.9 | 20.62 |
| Tellurite resistance protein tehB | b1430 | 3.76 | 3.60 | Anaerobic nitric oxide reductase flavorubredoxin norV | b2710 | 1.49 | 10.46 |
| N-hydroxyarylamine O-acetyltransferase nhoA | b1463 | 0.35 | 2.83 | Nitric oxide reductase FlRd-NAD(+) reductase norW | b2711 | 1.16 | 4.13 |
| Respiratory nitrate reductase 2 gamma chain narV | b1465 | 1.57 | 2.03 | Uncharacterized protein hypA | b2726 | 0.12 | 2.09 |
| Uncharacterized protein yneF | b1522 | 0.66 | 2.26 | Biodegradative arginine decarboxylase adiA | b4117 | 0.06 | 6.11 |
| Cysteine desulfuration protein sufE | b1679 | 1.03 | 2.02 | Fe-S cluster repair ytfE | b4209 | 67.25 | 19.52 |
| Cysteine desulfurase sufS | b1680 | 1.20 | 2.53 | | | | |
| FeS cluster assembly sufD | b1681 | 1.17 | 2.39 | | | | |
| Probable ATP-dependent transporter sufC | b1682 | 1.13 | 2.36 | | | | |
| FeS cluster assembly sufB | b1683 | 1.04 | 2.45 | | | | |
| FeS cluster assembly sufA | b1684 | 1.35 | 2.47 | | | | |

**Table S3** Microarray data comparing fold-expression of genes during anaerobic growth of WT and Δ*oxyR E.coli* on 10 mM nitrate or fumarate. Genes induced > 2-fold in the Δ*oxyR* strain on nitrate versus fumarate (p-value cutoff of 0.05) are included. The corresponding induction levels for WT are given. Genes are listed in the order of their b-number and have been arranged into operons (delineated by solid lines) via *E. coli* Entry Point.

**Table S4. Real–time PCR primers employed**

| | |
|---|---|
| yeaR-F | TTTCTGGAGGGAACACCGCAAACT |
| yeaR-R | ATCTCGGCTACGCTGATGAACACA |
| yoaG-F | ACTTCTGGCACCAGCAAAGTCATC |
| yoaG-R | TGACCGTCACCAATAACAGCAATGG |
| ytfE-F | GGTGTGACGTTATTGGTGGTGTGT |
| ytfE-R | AATGGAAAGCGAGCACGATGAAGC |
| hmp-F | TGACGCTCAAACCATCGCTACAGT |
| hmp-R | ATACGGTCGTAGAAATGGGCGGTT |
| fdnG-F | ATATCGTGCGCCAGGTTCTGACAA |
| fdnG-R | TAGCGTCACGGTCAGCTTTCATCA |
| hcp-F | TGACCTTCAGGATTTACTCATCGCGG |
| hcp-R | GATGATGCCGTATTCACGCGCTTT |
| fdnH-F | GCCTTCTCAGGTGCGTGATTACAA |
| fdnH-R | ACAGGCTTTACAGCCGATACAGGT |
| hcr-F | TGTGGACGATTTCCCTGATTTGCC |
| hcr-R | TTCGCACGCTGACCAGTGCATATT |
| ymgA-F | GGAAGATGCTTTCCGACGCGATTT |
| ymgA-R | TTCTTCGGTTTGGCCCTCCTGAAT |
| ycgZ-R | TGCATACTCAGCAGGAAACTCTCG |
| ycgZ-R | TTGGCACAAAGCGACTTTCGACTC |
| fdoG-F | TCGCGGAAACCCGGCAGTATAAA |
| fdoG-R | AGCCCACAGCCTACGGAACAATA |
| ymgC-F | AAATCTCGAGAGGGAGGTGTTCATGACG |
| ymgC-R | ACGCAAGCGTAAAGCCTGATCAAT |
| yeaR-F | AACACAATAACGTTCGCCCGTTGG |
| yeaR-R | ATTCGTTGCGGTAACTGTGATGCC |
| tauA-F | CGATTGAAGTCTTCTTGCTGGCGT |
| tauA-R | TGCGTTTGCCAATCAGATCTTCCG |
| ogt-F | AATGGGAAGAGTACAGCGAACGCA |
| ogt-R | TTGGTGGCAGAAATGCGCTCATAG |
| fdnI-F | TTATTGATCGCGCCTGTCACTGGA |
| fdnI-R | CAGCGTCGGGAAGAAGAACGAAAT |
| cyoD-F | AGTGGTACAGGTTCTGGTGCATCT |
| cyoD-R | AAGACAAACGCCGTCATGTTCCAG |
| dadA-F | TGTCATACTGGGAAGTGGTGTGGT |
| dadA-R | GGTGACCTCATGTCCTGCCTGATTTA |
| yeaC-F | ATGATGCCTGAGGTATACCAGCGT |
| yeaC-R | TTTGTTCCTCGGTCAACGCAACG |
| ilvA-F | ATTCTGGTGAAGCGCGAAGATCG |
| ilvA-R | TGCGCTTTCTGTTCTTCCGTCA |

**Supplemental References**


28. T. Baba *et al.*, *Mol Syst Biol* **2**, 2006 0008 (2006).
29. M. Feelisch, J. S. Stamler, *Methods in Nitric Oxide Research*. (Wiley, New York, 1996), pp. 455-478.
30. J. S. Stamler *et al.*, *Proc Natl Acad Sci U S A* **89**, 7674 (1992).
31. S. R. Jaffrey, H. Erdjument-Bromage, C. D. Ferris, P. Tempst, S. H. Snyder, *Nat Cell Biol* **3**, 193 (2001).
32. M. T. Forrester *et al.*, *Nat Biotechnol* **27**, 557 (2009).
33. G. Storz, S. Altuvia, *Methods Enzymol* **234**, 217 (1994).
34. H. Xu, M. A. Freitas, *BMC Bioinformatics* **8**, 133 (2007).